IOP Conf. Series: Journal of Physics: Conf. Series **881** (2017) 012003 doi:10.1088/1742-6596/881/1/012003

Finite element modelling of acoustic emission sensor

S I Gerasimov[1,2] **and T V Sych**[3]

[1] Professor, Department of Structural Mechanics, Siberian Transport University, Novosibirsk, Russia
[2] Professor, Tomsk Polytechnic University, Tomsk, Russia
[3] Research Assistant, Siberian Transport University, Novosibirsk, Russia

E-mail: 912267@gmail.com

Abstract. With a validated finite element system COSMOS/M, the out-of-plane displacements corresponding to model sources of acoustic emission (AE) were calculated in three-dimensional samples. The displacement signals were calculated for positions of the receiver on the top plate surface at several different distances (in the far-field) from the source's epicenter.

1. Introduction

The optical, acoustical non-destructive technologies are widely used in field testing of high-pressure vessels, pipelines, and castings [1-5]. The AE-sensor constitutes the first part in an AE measurement chain and therefore is of particular importance [6]. A subsequent measurement system can only process the signals that the AE-sensor does pick up. The AE-sensor converts the surface movement caused by an elastic wave into an electrical signal which can be processed by the measurement equipment. In [7] the models of a single piezoelectric ceramics with the arrival of longitudinal and transverse waves on it have been considered. The results were obtained and the analysis of the processes occurring when longitudinal and transverse waves arriving on a piezoceramic plate with a 3:1 aspect ratio has been performed.

The piezoelectric element of the AE-sensor should pick up the faintest surface movements (i.e. have high sensitivity) and convert these movements most efficiently to an electric voltage.

In this paper we are modelling a multilayer sensor. The main three elements of an acoustic-emission transducer are selected: technical ceramics, piezoelectric ceramics, and damping element. Also we are analysing the behaviour of the piezoelectric plate under the influence of the two kinds of waves - longitudinal and transversal. In the former case the response of the model against the front of the acoustic wave applied normal to the site of the piezoelectric plate that simulates the arrival of the longitudinal wave is analysed. In the latter case the response of the same model, but against the front tangential movement that simulates the arrival of transverse waves is analysed.

2. Acoustic emission sensor modelling

The main structural elements of the acoustic AE-sensor (AES) are the piezoelectric ceramics, the technical ceramics, and the damping element (see figure 1). To analyze the processes taking place in the AES when an acoustic-emission wave arrives, the Model is considered, which consists of three layers.

The lower layer of the Model had a height of 1 mm and the properties of the technical ceramics, which in real devices protects the AES from impact and wear. For the middle layer of the 5-mm-thick Model, the physical and mechanical properties of the piezoelectric ceramics were specified. The upper layer of the Model had the physical and mechanical properties of the damping element. The physical and mechanical properties of the three layers are presented in table 1

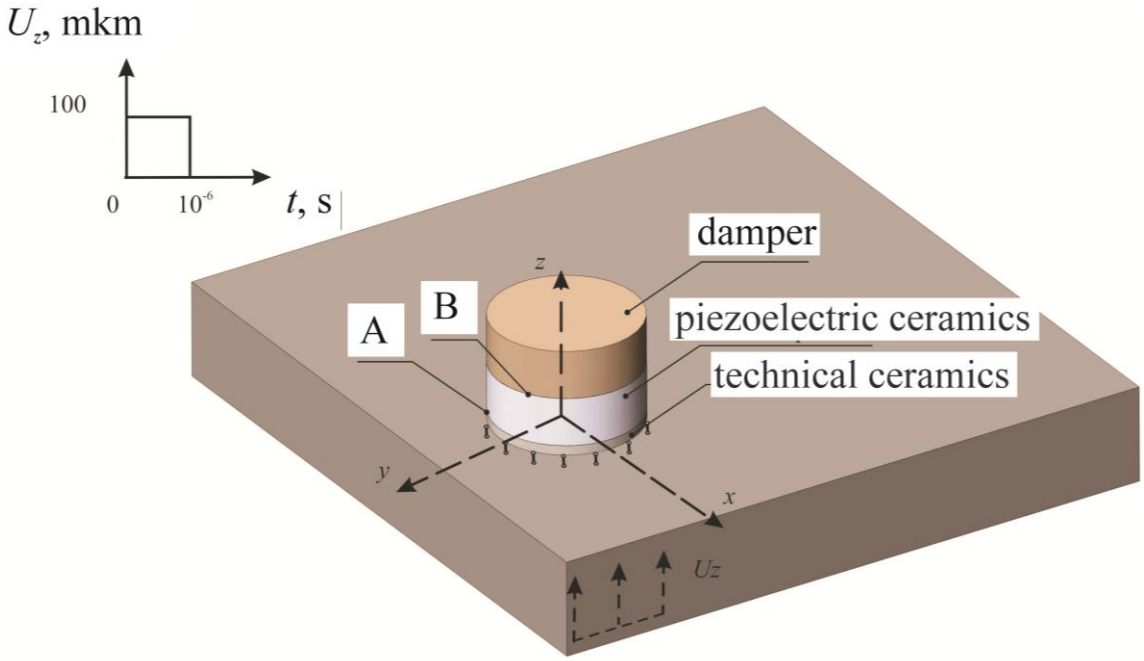

Figure 1. The structure of AE-sensor.

The boundary conditions for the Model are shown in figure 1. On the edge of the face A, the prohibition of displacements along the *z*-axis is introduced, in the two edges of the edge, displacements along the *x* axis and rotations relative to the *x*, *y*, *z* axes are ensured.

Table 1. Elastic properties of the materials used in FEM cases.

	Elastic modulus *E*, MPa	Poisson ratio ν	Density ρ, 10^3 kg/m^3	Wavelength λ_{min}, mm	Velocity of a longitudinal wave C_l, m/s
Material 1 (technical ceramics)	$2.2 \cdot 10^5$	0.22	2.3	10	9780
Material 2 (piezoelectric ceramics)	$1.2 \cdot 10^5$	0.33	7.75	4	3935
Material 3 (damper)	6.1	0.49	1	0.08	78

To each node of face A, a displacement along the *z* axis is applied, modulo 100 μm in the form of a pulse with a duration of $1 \cdot 10^{-6}$ s (see figure 1). This effect simulates the arrival of a longitudinal acoustic wave on the piezoelectric plate. The displacement at each node is applied along the normal to the plate surface. The calculation of the Model was performed in the nonlinear dynamic calculation module of the COSMOS/M software package. In the framework of the problem, the component U_z of the displacement of the nodes belonging to the face B and the difference in the displacements of the

faces A and B are analyzed. In fact, the displacements of the face B of the relative "zero" initial position along the *z* axis directly affect the output voltage of the converter.

The results of the calculation for different instants of time are shown in figure 2 a-n. The figure shows the distribution of displacements U_z in a fixed color scale - 200 ... 200 μm.

According to the theoretical calculations, the arrival time of the wave on the lower face of the piezoelectric ceramics is ~ $1 \cdot 10^{-7}$ s. Figure 2 *a* shows the distribution of displacements U_z at time $2.5 \cdot 10^{-7}$ s.

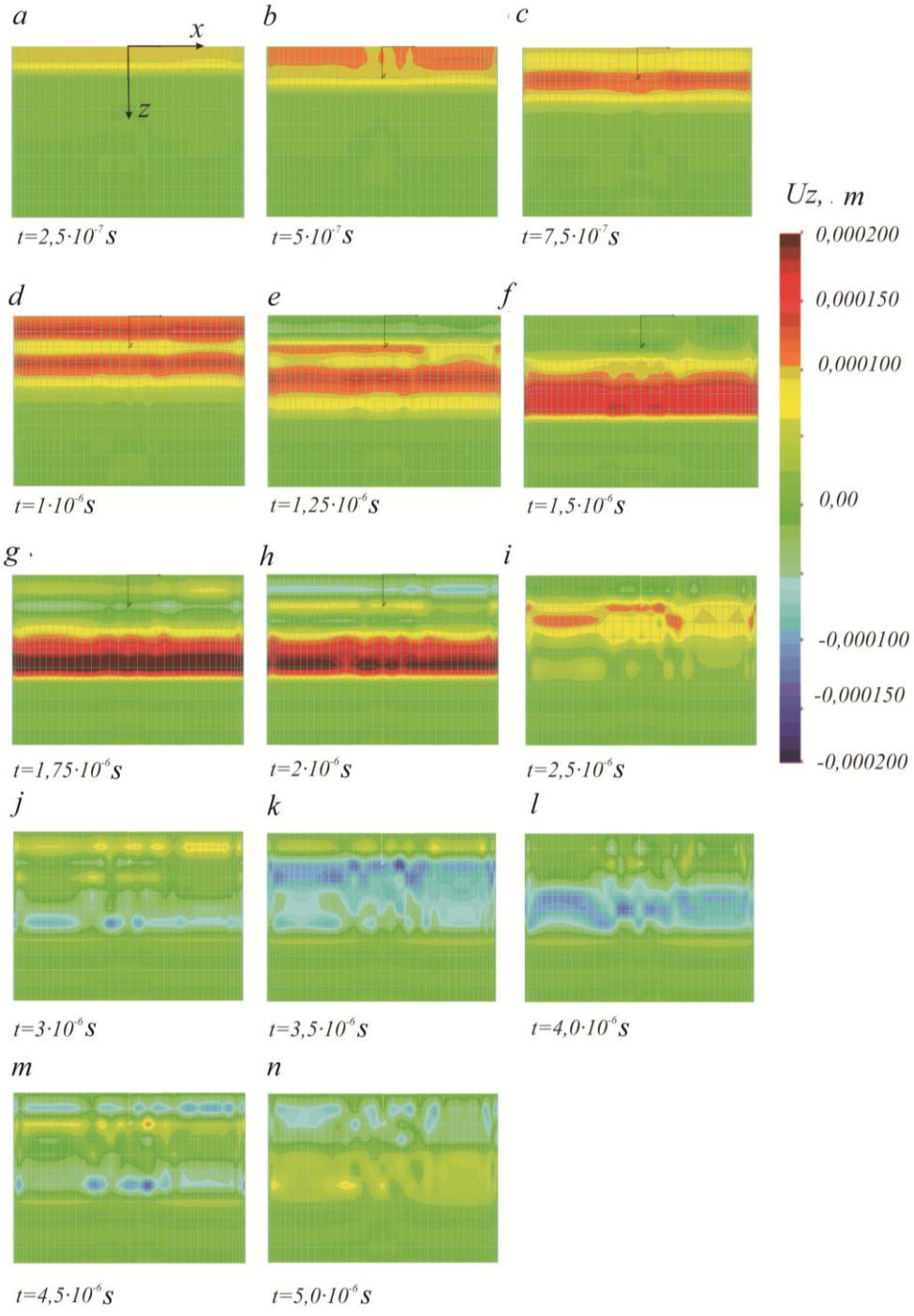

Figure 2. Displacements U_z for Model at different times (arrival of the longitudinal wave).

The wave front begins to spread from the face A, and passes the layer of technical ceramics. Then, the wave propagates through the layer of piezoelectric ceramics (see figures 2 b-c). At the time $7.5 \cdot 10^{-7}$ s in figure 2 c, the wave reaches the middle of the piezoelectric ceramics, and on the same figure the front of the reflected wave is seen from the layer boundaries. According to the theoretical calculation, the time of propagation of a wave through the piezoelectric ceramics layer of 5 mm is $1.3 \cdot 10^{-6}$ s. At the time points $1 \cdot 10^{-6}$ s and $1.25 \cdot 10^{-6}$ s, the main wave front reaches the upper face of the piezoelectric ceramics, and the fronts of the reflected waves are also visible. At the time points of $1.5 \cdot 10^{-6}$ s, $1.75 \cdot 10^{-6}$ s, and $2.0 \cdot 10^{-6}$ s, the maximum displacements of the upper face of the piezoelectric ceramics are observed. At the time point of $2.0 \cdot 10^{-6}$ s, the wave partially passes into the damper layer and begins to propagate through it at a very low rate.

The main wave is reflected from the upper face of the piezoelectric ceramics and goes in the opposite direction. At the same time, a layer with displacement movements in the lower layer of the model in the field of technical ceramics is already observed.

At the time $2.5 \cdot 10^{-6}$ s, the wave, reflected from the top face of the model, propagates in the opposite direction. At the time point $3.0 \cdot 10^{-6}$ s (figure 2 j) there is a stretching zone at the top of the piezoelectric ceramics. At the time $3.5 \cdot 10^{-6}$ s on figure 2 k the entire piezoelectric ceramics plate is in a stretched state. At the time point of $4.5 \cdot 10^{-6}$ s, the reflections in technical ceramics and the piezoelectric ceramics are visible. By the time $5.0 \cdot 10^{-6}$ s, as a result of the re-reflections, there are two zones of expansion and compression in the upper and lower zones of the Model.

The following figure 3 shows the distribution of displacements U_z as a function of the node numbers n ranging from 1 to 441 are given along the horizontal axis. To estimate the signal level, the difference ΔU_z between displacements the upper and lower faces of Model is taken. The results are presented for different instants of time: $0.5 \cdot 10^{-6}$ s, $1.0 \cdot 10^{-6}$ s, $1.25 \cdot 10^{-6}$ s, $1.5 \cdot 10^{-6}$ s, $1.75 \cdot 10^{-6}$ s. For the sake of clarity of the results obtained, a uniform displacement scale from minus 200 μm to plus 250 μm is chosen. On the displacements distribution graph for times of $0.5 \cdot 10^{-6}$ s, and $1.0 \cdot 10^{-6}$ s, it is seen that ΔU_z is negative - the lower face is stretched, and the upper face displacements are close to zero. At the time instants of $1.25 \cdot 10^{-6}$ s, $1.5 \cdot 10^{-6}$ s, $1.75 \cdot 10^{-6}$ s, the difference ΔU_z gradually increases and passes into the region of positive values - at those moments the wave reaches the upper plane and stretches this part of EA-sensor. This can be observed on figure 3, while the ΔU_z value reaches its maximum.

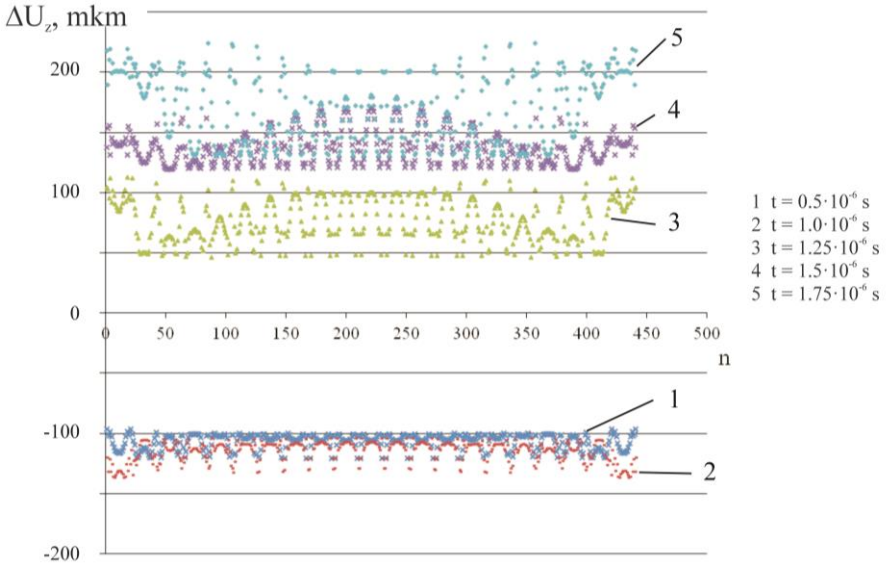

Figure 3. Distribution of the displacement difference ΔU_z of the upper and lower faces.

The summary results of the displacements $U^{\Sigma} = \sum U_z$ of the upper face nodes of the Model at various times are shown in table 2.

Table 2. Total displacement, m.

t, 10^{-6} s	U^{Σ}, m
0,5	$-4{,}71 \cdot 10^{-2}$
1,00	$-5{,}07 \cdot 10^{-2}$
1,25	$3{,}42 \cdot 10^{-2}$
1,50	$6{,}07 \cdot 10^{-2}$
1,75	$7{,}52 \cdot 10^{-2}$

3. Summary

As a result of numerical experiments, it is shown that the arrival of the longitudinal wave transducer on the sensor element leads to the maximum total displacements of the upper face and, accordingly, to a stable output signal on the piezoelectric plate. At the same time, the arrival of a transverse wave on the sensor element of the transducer leads to a mode of oscillations, at which the total displacements of the upper face are practically equal to zero. This, in turn, leads to a low output signal.

Based on the results of the work, the following recommendations are established: acoustic emission converters should be installed at the places of the monitored object, where the normal component of displacements is maximum.

References

[1] Builo S I 2004 Diagnostics of deformational and fracture stages based on integral parameters of the flow of acoustic-emission acts *Russian Journal of Nondestructive Testing* **40(8)** 552
[2] Gerasimov S I , Zhilkin V A 2006 Contact holographic interferometer for studying the deformation of small-curvature shells of revolution *Journal of Applied Mechanics and Technical Physics* **47(3)** 455
[3] Yurchenko A, Syriamkin V, Okhorzina A, Kurkan N 2015 PV effectiveness under natural conditions *IOP Conf. Ser.: Materials Science and Engineering* **81(1)** 012097
[4] Gerasimov S I, Zhilkin V A 1988 Investigation of plane elastic-plastic problems by the holographic interferometry methods *Journal of Applied Mechanics and Technical Physics* **29(2)** 260
[5] Hamstad M 2007 Acoustic emission source location in a thick steel plate by Lamb modes *Journal of Acoustic Emission* **25** 194
[6] Sych T, Gerasimov S, Kuleshov V 2012 Simulation of the propagation of acoustic waves by the finite element method *Russian Journal of Nondestructive Testing* **48(3)** 147
[7] Gerasimov S, Sych T, Kuleshov V 2016 Application of finite elements method for improvement of acoustic emission testing *Journal of Physics: Conference Series* **671** 012017